npg

ORIGINAL ARTICLE

Syndecan-1 promotes the angiogenic phenotype of multiple myeloma endothelial cells

S Lamorte[1], S Ferrero[2], S Aschero[2], L Monitillo[2], B Bussolati[1], P Omedè[2], M Ladetto[2] and G Camussi[1]

Angiogenesis is considered a hallmark of multiple myeloma (MM) progression. In the present study, we evaluated the morphological and functional features of endothelial cells (ECs) derived from bone marrow (BM) of patients affected by MM (MMECs). We found that MMECs compared with normal BM ECs (BMECs) showed increased expression of syndecan-1. Silencing of syndecan-1 expression by RNA interference technique decreased *in vitro* EC survival, proliferation and organization in capillary-like structures. *In vivo*, in severe combined immunodeficient mice, syndecan-1 silencing inhibited MMEC organization into patent vessels. When overexpressed in human umbilical vein ECs and BMECs, syndecan-1 induced *in vitro* and *in vivo* angiogenic effects. Flow-cytometric analysis of MMECs silenced for syndecan-1 expression indicated a decreased membrane expression of vascular endothelial growth factor (VEGF) receptor-2 (VEGFR-2). Immunoprecipitation and confocal analysis showed colocalization of VEGFR-2 with syndecan-1. Absence of nuclear translocation of VEGFR-2 in syndecan-1-knockdown cells together with the shift from perinuclear localization to recycling compartments suggest a role of syndecan-1 in modulation of VEGFR-2 localization. This correlated with an *in vitro* decreased VEGF-induced invasion and motility. These results suggest that syndecan-1 may contribute to the highly angiogenic phenotype of MMECs by promoting EC proliferation, survival and modulating VEGF–VEGFR-2 signalling.

INTRODUCTION

Multiple myeloma (MM) is a haematological malignancy characterized by accumulation of clonal malignant plasma cells predominantly within the bone marrow (BM)[1] and by increased BM neovascularization.[2-4] There is a direct correlation between BM microvessel density and parameters of disease progression.[5] Moreover, increased BM vascularization in MM patients is correlated with a poor prognosis.[6-8] Endothelial cells (ECs) derived from MM patients significantly differ from normal microvascular ECs in terms of proliferation, phenotype, morphology and capillarogenic activity.[9-12] In patients affected by MM syndecan-1, a heparan sulphate proteoglycan, is overexpressed by myeloma cells in the BM and peripheral blood.[13,14] The high serum level of shed syndecan-1 has been associated with an unfavourable prognosis.[15,16] The presence of heparin sulphate chains allows cell-to-cell and cell-to-extracellular matrix interactions. Moreover, syndecan-1 is able to interact with several growth factors, including pro-angiogenic factors such as vascular endothelial growth factor (VEGF) and basic fibroblastic growth factor.[17] Syndecan-1 seems to be able to modulate neovascularization by increasing the local concentration of growth factors,[18] by mediating their binding to specific receptors[19-21] and/or by interacting directly with the receptors.[22-25] Expression of syndecan is often altered in cancer,[26,27] and several studies suggest that syndecan-1 expression promotes the growth of several malignancies, including MM.[28-31]

The aim of the present study was to investigate whether syndecan-1 was overexpressed on the surface of ECs derived from the BM of MM patients (MMECs) as compared with normal BM ECs (BMECs). Moreover, we investigated the functional implication of syndecan-1 expression by MMECs in MM angiogenesis. Using an RNA interference approach, to knockdown syndecan-1 expression, we determinate the involvement of syndecan-1 in MMEC proliferation, resistance to apoptosis, the ability to invade the basal membrane, *in vitro* (2012) **26,** 1082–1091. and *in vivo* angiogenic properties, and responsiveness to VEGF stimulation.

MATERIALS AND METHODS

Patients

BM aspirates were collected from 10 MM patients at diagnosis. All patients provided informed consent in accordance with local Institutional Review Board requirements and the Declaration of Helsinki. Patient's clinical features are shown in Supplementary Table 1.

Cell lines

Primary microvascular EC lines from the BM of healthy donor (BMECs) or MM patients (MMECs) were isolated. Briefly, BM aspirates were centrifuged on Ficoll (Biochrom AG, Berlin, Germany) gradient centrifugation and ECs were isolated from mononuclear cells by using anti-CD31Ab coupled to magnetic beads by magnetic cell sorting (MACS system, Miltenyi Biotec, Auburn, CA, USA). Cells were recovered and transferred to six-well plates, previously coated with Endothelial Cell Attachment Factor (Sigma, St Louis, CA, USA) in 3-ml complete medium per well. Primary cultures of human umbilical vein ECs (HUVECs) were isolated as described previously.[32] Cell

[1]Department of Internal Medicine, Research Center for Experimental Medicine (CeRMS) and Molecular Biotechnology Center, University of Torino, Torino, Italy and [2]Department of Oncology and Experimental Medicine; Division of Hematology, University of Torino, Torino, Italy. Correspondence: Dr G Camussi, Dipartimento di Medicina Interna, Ospedale Maggiore S Giovanni Battista, Corso Dogliotti 14, Torino 10126, Italy.
E-mail: giovanni.camussi@unito.it

types were maintained in culture with endothelial basal medium (EBM), completed with human epidermal growth factor, hydrocortisone and bovine brain extract (all from Cambrex Bioscience, Walkersville, MD, USA), with 10% fetal bovine serum (FBS).

Flow cytometry and immunofluorescence

Cell phenotype was studied by flow cytometry (FACSCalibur; Becton Dickinson, San Jose, CA, USA) as described under Supplementary Materials and methods. Immunofluorescence studies for phenotype characterization and confocal analysis of vascular endothelial growth factor receptor-2 (VEGFR-2) localization were performed as described under Supplementary Materials and methods.

Syndecan-1 overexpression

The pOTB7 plasmid, containing the full coding region of human *SDC1*, was purchased from Open Biosystems (Huntsville, AL, USA). The plasmid was purified according to the Qiagen Plasmid mini kit protocol (Qiagen GmbH, Hilden, Germany) and sent to Vector BioLabs (Philadelphia, PA, USA) for AD-FRP-h synedecan-1 adenoviral vector construction. For virus infection, BMECs or HUVECs were seeded at a density of 2×10^5 cells/well in six-well plates and infected with 0.5×10^6 IFU/p.f.u. (infectious unit/ml) of virus preparation. After overnight absorption at $37\,^\circ$C, the viral infection medium was removed, cells were washed twice with phosphate-buffered saline and fresh medium was added. Syndecan-1 overexpression was subsequently analysed by flow cytometry and quantitative reverse transcription-PCR (qRT-PCR).

Cell proliferation and apoptosis assays

Cell proliferation was assessed by 5-bromo-2′-deoxyuridine incorporation and apoptosis by TUNEL assay as described under Supplementary Materials and methods.

Apoptosis and cell-cycle arrays, and qRT-PCR

MMECs were compared with MMEC syndecan-1 small interfering RNA (siRNA) and BMECs by PCR arrays and qRT-PCR (see Supplementary Table 2) as detailed under Supplementary Materials and methods.

Matrigel invasion and cell adhesion assays

Details on Matrigel invasion and cell adhesion assays are provided under Supplementary Materials and methods.

Zymographic analysis

Gelatinolytic activity of matrix metalloproteinases (MMPs) was assessed under non-reducing conditions using a modified sodium dodecyl sulphate-PAGE. The supernatant, obtained after 24 h of starvation, was mixed with Laemmli buffer and loaded into an 8% polyacrylamide gel copolymerized with 1 mg/ml gelatin (Sigma). Electrophoresis and gel staining were performed as described previously.[33] An aliquot of RPMI with 10% FBS was used to determine the molecular weight of the gelatinase.

In vitro and in vivo angiogenesis assays

In vitro angiogenesis was studied by seeding cells on reduced growth factor Matrigel-coated plates and *in vivo* angiogenesis by subcutaneous injection of cells within Matrigel into severe combined immunodeficient (SCID) mice as described under Supplementary Materials and methods.

Immunoprecipitation

Cells were serum-starved for 24 h and then lysed in cold DIM buffer (50 mM Pipes (pH 6.8), 100 mM NaCl, 5 mM MgCl$_2$, 300 mM sucrose, 5 mM EGTA) plus 1% Triton X-100 and a mixture of protease inhibitors (Sigma). Equal amount (1 mg) of proteins was immunoprecipitated using protein-A/G plus–agarose beads (Santa Cruz Biotechnology) pre-coated by an anti-syndecan-1 or a VEGFR-2 monoclonal antibody (Santa Cruz Biotechnology, Santa Cruz, CA, USA) (each at 2 µg). Bound proteins were washed several times in DIM buffer

and resuspended in boiling Laemmli buffer. Resuspended proteins were then subject to electrophoresis on Any kD sodium dodecyl sulphate-polyacrylamide gel (Bio-Rad Laboratories, Hercules, CA, USA), transferred to nitrocellulose and probed with the appropriate antibody, followed by a horseradish peroxidase-conjugated secondary antibody (Sigma) and an enhanced chemiluminescent substrate (Thermo Scientific, Waltham, MA, USA).

EC migration assays

Details on EC migration assays are provided under Supplementary Materials and methods.

RESULTS

Isolation and characterization of MMECs

MMECs and BMECs were isolated, respectively, from BM aspirates of 10 different MM patients at diagnosis and four different healthy donors. Flow-cytometric analysis showed that all the cell lines isolated were endothelial; more than 95% cells expressed UEA-1, VWF and CD144 (VE-cadherin) but not monocyte–macrophage (CD14), leukocyte (CD45), plasma cell (CD38) markers and mesenchymal cell markers (vimentin) (Figures 1a and b). The MMECs phenotype was analysed in comparison with BMECs (Supplementary Table 3). Both cell types expressed the same levels of CD44, CD90, CD29, CD105, CD144 (VE-cadherin), CD146, VEGFR-1 and VEGFR-3 and showed absence of CD154, CD34 and CD133 expression. MMECs showed greater expression of CD40, UEA-1, VEGFR-2 and, in particular, CD138 (syndecan-1) than BMECs (Supplementary Table 3). The higher expression of syndecan-1 by MMECs was not only at the protein level but also at the mRNA level, as confirmed by qRT-PCR (Figures 1c and d). At variance between MMECs and BMECs, HUVECs did not express syndecan-1 protein and mRNA. For this reason HUVECs were used as control for studies aimed to investigate the function of syndecan-1.

Syndecan-1 expression promotes proliferation and protects against apoptosis

To analyse the role of syndecan-1 expression on MMECs, we used an RNA interference approach. A pool of syndecan-1 siRNAs and, as control, an scr-siRNA was transiently transfected into MMECs to knock down syndecan-1 expression. Syndecan-1 siRNA, but not scr-siRNA, transfection effectively inhibited syndecan-1 mRNA and protein expression in MMECs (see Supplementary Figure 1 and Supplementary Materials and methods). Then, to study the effect of syndecan-1 knockdown on EC apoptosis and proliferation, we compared the growth and apoptosis resistance of MMECs using an MMEC syndecan-1 siRNA and, as control, an MMEC scr-siRNA. An additional control included HUVECs. As shown in Figure 2a, after 48 h of culture with decreasing serum levels, MMECs proliferated significantly more than HUVECs. Transfection with syndecan-1 siRNA, but not scr-siRNA, reduced this increase to levels comparable to that of HUVECs. As internal control, cells were grown in culture media (EBM 10% FBS) (Figure 2a). Moreover, to evaluate the effect of syndecan-1 expression on apoptosis resistance, HUVECs, MMECs, MMEC syndecan-1 siRNA and, as control, MMEC scr-siRNA, were grown for 24 h in the absence of serum (Figure 2b). As shown in Figure 2b, MMECs showed less sensitivity to apoptosis, induced by serum deprivation, compared with HUVECs. Knockdown of syndecan-1 expression (MMEC syndecan-1 siRNA) determinated an increase in sensitivity to apoptosis, even in the presence of serum. These results suggest that expression of syndecan-1 on MMECs has a role in cell proliferation and resistance to apoptosis. These effects seemed to be independent from a reduced cell adhesion of syndecan-1-knockdown cells, as both MMECs and MMEC syndecan-1 siRNA showed the same ability to adhere to gelatin-coated plates on which proliferation and apoptosis assays were performed (data not shown).
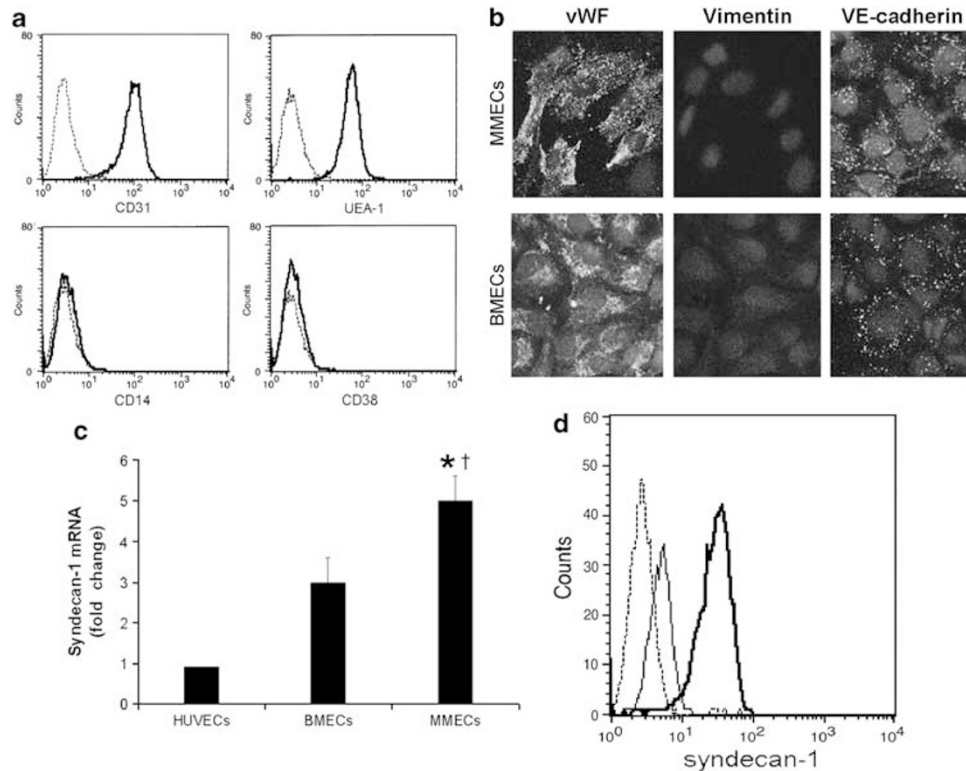
Figure 1. Characterization of HUVECs, BMECs and MMECs assessed by flow-cytometric, immunofluorescence and qRT-PCR analysis. (**a**) Representative flow-cytometric analysis showing isolated MMECs expressing CD31 and ulex europaeus agglutinin-1 (UEA-1) but not CD14 and CD38. The flow-cytometric histograms are representative of six independent experiments with similar results. The dark lines represent the MMECs and the dotted lines represent the corresponding isotype control antibody. (**b**) Representative confocal micrographs of vWF, vimentin and VE-cadherin expression in BMECs and MMECs detected by immunofluorescence. Original magnification: ×400. (**c, d**) Comparison of syndecan-1 mRNA expression by HUVECs, BMECs and MMECs using qRT-PCR (**c**) and flow cytometry (**d**). (**c**) The normalized expression of the genes with respect to *ACTB* was computed for all samples. Values are expressed as fold change with respect to HUVECs and are the mean ± s.d. of six independent experiments performed in triplicate. Student's *t*-test was performed (*$P<0.001$ MMECs versus HUVECs; $^{\dagger}P<0.05$ MMECs versus BMECs). (**d**) Representative flow-cytometric analysis showing syndeacan-1 expression in HUVECs (dotted line), BMECs (thin line) and MMECs (dark line). The flow-cytometric histograms are representative of six independent experiments with similar results.

To explore the mechanism involved in proliferation inhibition and apoptosis induction by syndecan-1 silencing, we investigated, by PCR arrays, human cell-cycle and apoptosis pathways. The results showed changes in genes involved in G_2/M transition and the M phase. GTP-binding RAS-like-3 was highly expressed by syndecan-1-knockdown cells as compared with MMECs, whereas, the levels of baculoviral inhibitor of apoptosis repeat containing-5 (BIRC5), cyclin-B1 (CCNB1), CDC28 protein kinase-regulatory subunit-1B (CKS1B), CDC28 protein kinase-regulatory subunit-2 (CKS2), cyclin-B2 (CCNB2), cyclin-dependent kinase-1 (CDK1), cell division cycle-20 homologue (CDC20) and antigen identified by monoclonal antibody Ki-67 (MKi67) were decreased. These genes were verified by qRT-PCR and were all significantly changed as compared with MMECs (Figure 3a). These results indicated an arrest of syndecan-1-knockdown cells in G_2/M transition and in the M phase. The apoptosis array revealed that syndecan-1-knockdown cells expressed elevated level of pro-apoptotic genes such as BCL2-associated X protein (BAX) and tumor necrosis factor receptor superfamily member-21 (TNFRSF21), whereas anti-apoptotic genes, such as BCL2-like-10 (BCL2L10), baculoviral inhibitor of apoptosis repeat containing-3 (BIRC3) and nucleolar protein-3 (NOL3) were downregulated. qRT-PCR confirmed significant variation of BAX, TNFRSF21, BCL2L10, BIRC3 and NOL3 expression (Figure 3b). Interestingly, syndecan-1-knockdown cells had low expression of BIRC3, whose encoded protein inhibits apoptosis induced by serum deprivation. This suggests that low membrane expression of syndecan-1 sensitizes the cells

to apoptosis induced by serum deprivation. The profile of gene analysis of BMECs, when compared with that of MMECs, showed a significant reduction of genes involved in M phase and a decrease of anti-apoptotic genes and increase of pro-apoptotic genes (Figures 3a and b).

Syndecan-1 expression promotes Matrigel invasion
We analysed MMEC basal membrane invasiveness and its dependence on syndecan-1 expression. Thus, we compared HUVECs, MMECs, MMEC syndecan-1 siRNA and, as control, the MMEC scr-siRNA for ability to invade Matrigel *in vitro*. The results showed that MMECs, as compared with HUVECs, showed enhanced ability to invade Matrigel, whereas the MMEC syndecan-1 siRNA, but not the MMEC scr-siRNA, showed a statistically significant decrease of this ability (Figure 4a). To evaluate whether syndecan-1 expression correlated with MMP secretion, we tested the gelatinolytic ability of HUVECs, MMECs, MMEC scr-siRNA and MMEC syndecan-1 siRNA supernatants. MMECs, MMEC scr-siRNA and HUVECs secrete activated MMP-2 (72-kDa form) and MMP-9 (83-kDa form). The MMEC values were, on average, 3 and 4 times higher for MMP-2 and MMP-9, respectively, as demonstrated previously[11] and there were no differences between MMECs and MMEC scr-siRNA (data not shown). We detected a decrease in both the 72 and 83-kDa bands of about 1.5 and 3 times, respectively, in the MMEC syndecan-1 siRNA supernatant as compared with the MMEC supernatant (Figure 4b). The presence
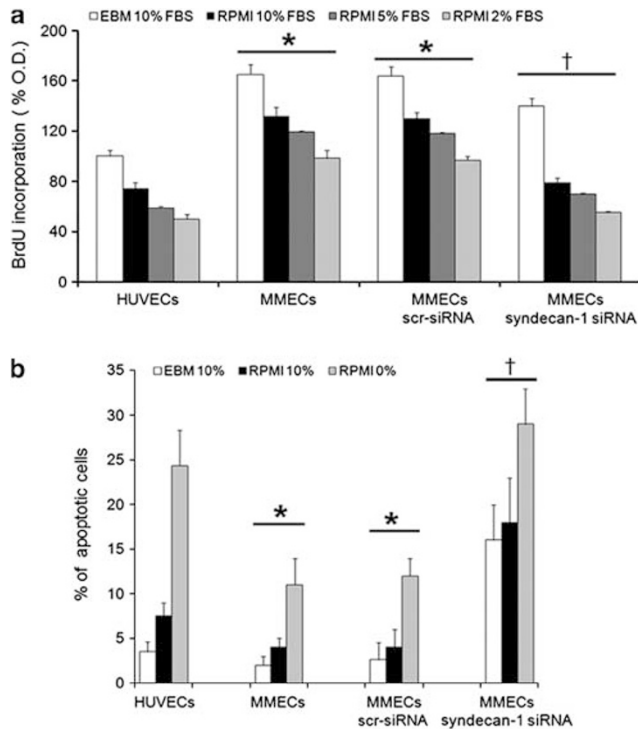
Figure 2. Syndecan-1 expression is associated with apoptosis resistance and enhanced cell proliferation. (**a**) Cell proliferation after 48 h of incubation in decreasing serum concentrations: RPMI 10% FBS (black bars), 5% FBS (grey bars) and 2% FBS (light grey bars), and, as control, culture media (complete EBM 10% FBS, white bar). Data are expressed as the mean ± s.d. of four experiments performed in triplicate. Analysis of variance with Dunnett multiple comparison test was performed (*$P < 0.01$ MMECs versus HUVECs; [†]$P < 0.05$ MMEC syndecan-1 siRNA versus MMECs). (**b**) Apoptosis after 24 h of incubation in the presence (black bars) and absence of serum (grey bars), and, as control, in culture media (complete EBM 10% FBS, white bars). Data are expressed as the mean ± s.d. of four experiments performed in triplicate. Analysis of variance with Dunnett multiple comparison test was performed (*$P < 0.001$ MMECs versus HUVECs; [†]$P < 0.001$ MMEC syndecan-1 siRNA versus MMECs).

Figure 3. Cell-cycle and apoptosis-related genes are modulated in syndecan-1-knockdown cells. Expression profile of genes involved in proliferation (**a**) and apoptosis (**b**) of MMEC syndecan-1 siRNA as compared with MMECs and BMECs by qRT-PCR. The normalized expression of the genes with respect to gylceraldehyde-3-phosphate dehydrogenase (*GAPDH*) was computed for all samples. Values are expressed as fold change with respect to MMECs and are the mean ± s.d. of three independent experiments performed in triplicate. Student's *t*-test was performed (*$P < 0.05$ MMECs syndecan-1 siRNA versus MMECs; [†]$P < 0.05$ BMECs versus MMECs).

of reduced invasion and decrease of the active form of MMP-2 and MMP-9 in MMEC syndecan-1 siRNA suggests a possible role of syndecan-1 in the regulation of MMP secretion and *in vitro* MMEC invasion ability. Syndecan-1 can promote cell adhesion and invasion into the BM extracellular matrix.[34] In this contest we analysed MMECs and MMEC syndecan-1 siRNA ability to adhere to Matrigel. After 2 h of incubation the MMEC syndecan-1 siRNA showed decreased adhesion of about 40% compared with MMECs (Figure 4c).

Syndecan-1 expression promotes *in vitro* and *in vivo* angiogenesis
When plated on growth factor-reduced Matrigel in the absence of angiogenic stimulation, MMECs (Figure 5a, top right) formed an extensive network of ring-like structures, whereas BMECs (Figure 5a, top left, and Figure 5b) and HUVECs (Figure 5b) showed a less organized vascular network. To evaluate whether this enhancement was correlated with syndecan-1 expression, we compared the ability of HUVECs, BMECs, MMECs, MMEC syndecan-1 siRNA and, as control, MMEC scr-siRNA to form *in vitro* capillary-like structures (Figures 5a and b). Syndecan-1 knockdown significantly inhibited the formation of vessel-like structures both at 5 and at 24 h (Figure 5a, bottom left, and Figure 5b). By contrast, transfection with a control siRNA, MMEC scr-siRNA, did not affect
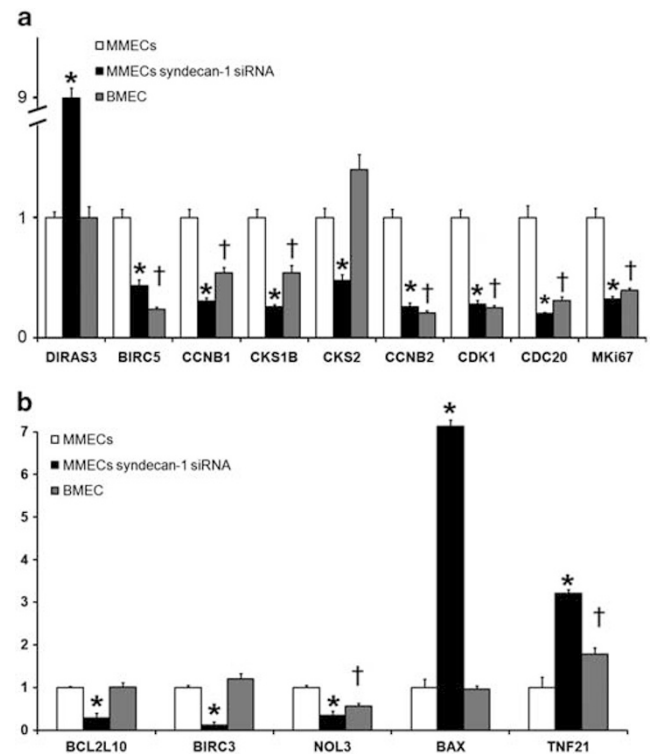
the endothelial organization (Figure 5a, bottom right, and Figure 5b). Moreover, we evaluate the involvement of syndecan-1 expression in the *in vivo* angiogenesis. For *in vivo* experiments MMECs were transfected with syndecan-1 short-hairpin RNAs (shRNAs) (MMEC syndecan-1 shRNA) to obtain a more stable reduction of syndecan-1 expression and, as control, with an scr-shRNA (MMEC scr-shRNA) (see Supplementary Figure 1 and Supplementary Materials and methods). HUVECs, BMECs, MMECs, MMEC syndecan-1 shRNA and, as control MMEC scr-shRNA were injected subcutaneously within Matrigel in SCID mice. Seven days after injection MMECs and to a less extent BMECs, but not HUVECs, were able to organize in vessels connected with the murine vasculature as shown by the presence of erythrocytes in the lumen (Figure 5c, top right and left, and Figure 5e). Reduction of syndecan-1 expression (MMEC syndecan-1 shRNA) was associated with a significant reduction of this ability (Figure 4c, bottom left, and Figure 5e). By contrast, transfection with an shRNA control, MMEC scr-shRNA, did not affect the ability of MMECs to form a vascular structure *in vivo* (Figure 5c, bottom right, and Figure 5e). The human nature of implanted MMECs was assessed by immunofluorescence staining for human CD31 and human leukocyte antigen class-I (Figure 5d, left and right). Similar results were obtained for BMECs (data not shown). Thus, inhibition of syndecan-1 expression on MMECs was associated with a significant reduction of angiogenesis *in vitro* and *in vivo*, underlying the role of this protein in the MMEC angiogenic properties.
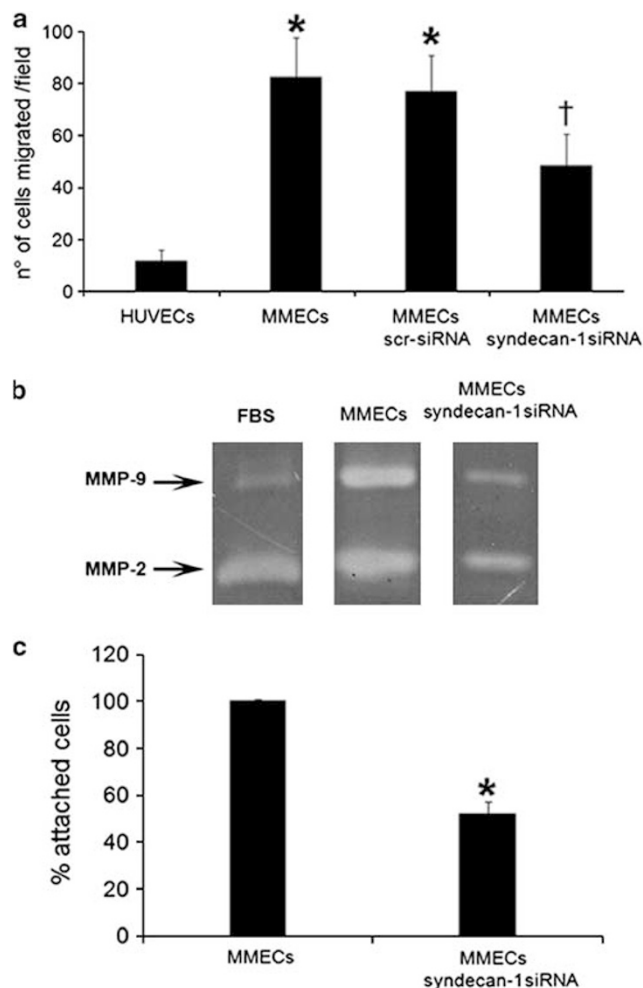
Figure 4. Syndecan-1 expression is associated with invasion properties of MMECs. (**a**) Invasion of HUVECs, MMECs and MMEC syndecan-1 siRNA and, as control, MMEC scr-siRNA towards Matrigel-coated filters were evaluated. Cells that migrated to the underside of the filters were counted in five microscope fields in each well at × 100 magnification. Data are expressed as the mean ± s.d. of four experiments performed in duplicate. Analysis of variance with Dunnett multiple comparison test was performed (*$P < 0.001$ MMECs versus HUVECs; $^{†}P < 0.001$ MMEC syndecan-1 siRNA versus MMECs). (**b**) Representative zymographic analysis of MMECs and MMEC syndecan-1 siRNA. The first lane (FBS) shows the control RPMI supplemented with 10% FBS. The clear bands represented gelatinase activity. Four experiments were performed with similar results. (**c**) Evaluation of MMECs and MMEC syndecan-1 siRNA attachment on growth factor-reduced Matrigel after 2 h in media used for invasion assay (not complete EBM with 10% FBS). Data are expressed as ± s.d. of three different experiments each in triplicate. Student's *t*-test was performed (*$P < 0.001$).

Acquisition of syndecan-1 expression stimulates angiogenesis *in vitro* and *in vivo*

To confirm the role of syndecan-1 in the enhanced *in vitro* and *in vivo* angiogenic properties of MMECs, we overexpressed syndecan-1 in HUVECs (AD-FRP h-syndecan-1 HUVECs) and BMECs (AD-FRP h-syndecan-1 BMECs) with an adenovirus coding the full sequence of human syndecan-1 and, as control, with an empty adenovirus (AD-FRP HUVECs, AD-FRP BMECs). qRT-PCR and flow-cytometric analysis showed that AD-FRP h-syndecan-1 HUVECs and BMECs overexpressed syndecan-1 mRNA and protein (Figures 6a and b). We compared the ability of uninfected HUVECs and

BMECs with AD-FRP h-syndecan-1 HUVECs and AD-FRP h-syndecan-1 BMECs to form capillary-like structures *in vitro* in the absence of angiogenic stimulus. After 5 h the extent of capillary-like structure on Matrigel was significantly enhanced in AD-RFP h-syndecan-1 HUVECs and AD-FRP h-syndecan-1 BMECs as compared, respectively, with uninfected HUVECs and BMECs (Figures 6c and d). We did not measure any statistical difference between uninfected and control cells (data not shown). Then, we evaluated the effect of subcutaneous injection in SCID mice of HUVECs and BMECs overexpressing syndecan-1 within Matrigel. After 7 days, massive angiogenesis was observed with aneurysm-like structures in mice injected subcutaneously with AD-FRP h-syndecan-1 HUVECs or AD-FRP h-syndecan-1 BMECs (Figure 6e, right), but not with AD-FRP HUVECs or AD-FRP BMECs (Figure 6e, left). The human origin of vessels formed by AD-FRP h-syndecan-1 HUVECs was verified by immunofluorescence for human CD31 and human leukocyte antigen class-I (Figure 6f, left and right). Similar results were obtained for AD-FRP h-syndecan-1 BMECs (data not shown). The areas of capillaries and aneurysm-like structures penetrating the Matrigel plugs were quantified in relation to the total Matrigel area. The percentage of vessel-like areas was significantly increased in AD-FRP h-syndecan-1 HUVECs or AD-FRP h-syndecan-1 BMECs as compared with AD-FRP HUVECs or AD-FRP BMECs (Figure 6g) We did not measure any statistical difference between uninfected and control cells (data not shown).

Syndecan-1 expression mediates VEGF–VEGFR-2 signalling

Analyzing the phenotype of MMECs versus syndecan-1-knock-down MMECs we found that syndecan-1 silencing determined a decrease in the expression of VEGFR-2 (Figure 7Aa). Conversely, induced syndecan-1 overexpression on BMECs and HUVECs increased VEGFR-2 protein expression (Figure 7Ab and c). Thus, we analysed the possibility that sydecan-1 could physically interact with VEGFR-2 and form an active complex at the membrane of MMECs. We observed that an anti-syndecan-1 antibody was able to precipitate two proteins of about 200 and 230 kDa, respectively, corresponding to two of the three isoforms of VEGFR-2, as shown by anti-VEGFR-2 immunoblots (Figure 7B, top). The specificity of this interaction was demonstrated by co-immunoprecipitation experiments using an antibody against VEGFR-2 (Figure 7B, bottom). Colocalization between VEGFR-2 and syndecan-1 in MMECs was also observed also by confocal microscopy (Figure 7C). These results indicated that syndecan-1 was associated to VEGFR-2. We then hypothesized that VEGFR-2 localization might be regulated by syndecan-1 expression. As seen by flow-cytometric analysis (Figure 7Aa) and confocal microscopy (Figure 7C), syndecan-1 silencing decreased the surface expression of VEGFR-2. As shown by immunofluorescence in permeabilized cells, the intracellular distribution of VEFGR-2 in MMECs was predominantly peri-nuclear, whereas in syndecan-1-knockdown cells it was cytoplasmic (Figure 7D) and colocalized with Ras-related in brain-11 (Rab11), a marker of the long-loop recycling pathway (Figure 7E). Similar results were observed with the Early Endosome Antigen-1 (EEA1) (data not shown). By contrast, in MMECs VEGFR-2, which was mainly perinuclear (Figure 7D), showed only minimal colocalization with the recycling markers (Figure 7E). No colocalization of VEGFR-2 was seen with either the Golgi Membrane protein-130 (GM130) or the marker of the Trans-Golgi Network-38 (TGN38) (data not shown). Moreover, nuclear translocation of VEGFR-2 after VEGF stimulation was almost completely abrogated in syndecan-1-knockdown cells (Figure 7F). A reduced synthesis of VEGFR-2 was also suggested by its reduced transcription as shown in Figure 7G.

Thus, we analysed the effect of syndecan-1 silencing in VEGF-induced motility. In basal condition, all cells analysed were found to remain steady for the whole period of observation, never exceeding an average speed of 11–13 ìm/h. Stimulation with VEGF
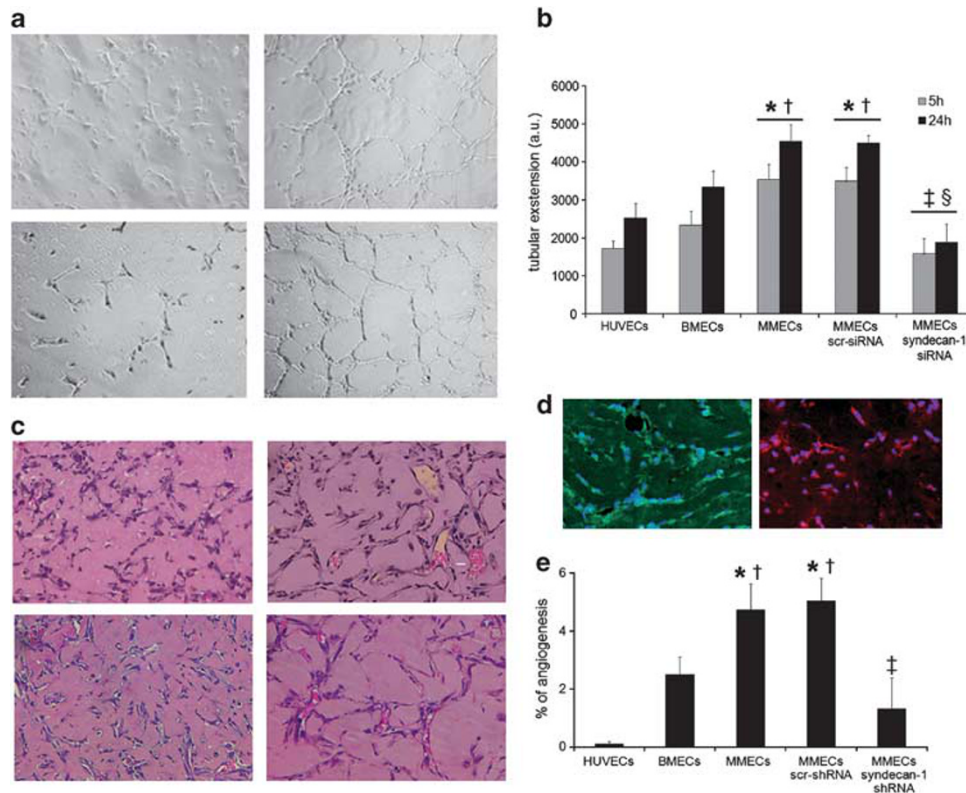
Figure 5. Effect of syndecan-1 expression on *in vitro* and *in vivo* MMEC angiogenesis. (**a**) Representative micrographs of capillary-like structure formation on Matrigel formed by BMECs (top left), MMECs (top right), MMEC syndecan-1 siRNA (bottom left) and MMEC scr-siRNA (bottom right) after 24 h of incubation. Original magnification, × 100. (**b**) Morphometric evaluation of capillary-like structures formed onto Matrigel after 5 h (grey bars) and 24 h (black bars). Data are expressed as the mean ± s.d. of the length of capillary-like structures evaluated, in arbitrary units by the computer analysis system, in six different experiments performed in triplicate. Analysis of variance with Newman–Keuls multi-comparison test was performed (*$P < 0.001$ MMECs and MMEC scr-siRNA versus HUVECs; [†]$P < 0.001$ MMECs and MMEC scr-siRNA versus BMECs; [‡]$P < 0.001$ MMEC syndecan-1 siRNA versus MMECs; [§]$P < 0.05$ MMEC syndecan-1 siRNA versus BMECs). (**c, d**) HUVECs, BMECs, MMECs, MMEC syndecan-1 shRNA and, as control, MMEC scr-shRNA within Matrigel were injected subcutaneously into SCID mice. Mice were killed after 7 days and Matrigel plugs were submitted for histological analysis. (**c**) Representative micrographs (haematoxylin/eosin staining) of Matrigel-containing BMECs (top left), MMECs (top right), MMEC syndecan-1 shRNA (bottom left) and MMEC scr-shRNA (bottom right). BMECs, MMEC syndecan-1 shRNA and MMEC scr-shRNA showed formation of vessels containing blood erythrocytes. Original magnification, × 200. (**d**) Representative confocal micrograph showing expression of human CD31 (left) and human leukocyte antigen class-I (right) on neo formed vessels in Matrigel by MMECs. Original magnification, × 400. (**e**) Quantitative evaluation of angiogenesis in a section of Matrigel plugs stained by haematoxylin/eosin staining. Angiogenesis was evaluated as the percentage of vessels area in five different fields at × 100 magnification. Only vascular structures containing red blood cells were counted as vessels. The data are the mean ± s.d. of five individual experiments. Analysis of variance with Newman–Keuls multi-comparison test was performed (*$P < 0.001$ MMECs and MMEC scr-shRNA versus HUVECs; [†]$P < 0.001$ MMECs and MMEC scr-siRNA versus BMECs; [‡]$P < 0.001$ MMEC syndecan-1 siRNA versus MMECs).

significantly enhanced HUVEC and MMEC migration (Figures 8a and b). In particular, MMECs showed a major response to the VEGF stimulus than HUVECs, as they reached a speed of approximately 26 μm/h, whereas HUVEC motility was about 19 μm/h. Knockdown of syndecan-1 expression on MMECs abrogated VEGF-dependent EC migration, reducing the speed average to basal levels (Figures 8a and b). The effects persisted for the whole period of observation (Figure 8a). Moreover, we analysed the effect of syndecan-1 knockdown on invasion in the presence of 25 ng/ml VEGF. After 48 h, both HUVECs and MMECs showed an increased ability to invade Matrigel in the presence of VEGF, as compared with the basal condition (Figure 8c). Conversely, syndecan-1 knockdown abrogated the VEGF-induced invasiveness of MMECs to levels comparable to that of HUVECs (Figure 6e).

DISCUSSION

In the present study, we found that ECs obtained from the BM of patients with MM overexpressed syndecan-1 and we provide

evidence that its expression contributes to their proliferative, apoptosis-resistant, pro-invasive and pro-angiogenic phenotype.

Previous studies suggested that overexpression of syndecan-1 by MM cells correlates with disease progression.[30,35-38] We here demonstrated that also MMECs overexpress this proteoglycan in respect to ECs derived from normal BM. As the functional significance of syndecan-1 expression by MMECs has not been investigated before, we examined its role in angiogenesis. It has been suggested that syndecan-1-retaining heparin-binding factors within the BM microenvironment may provide a support for the growth and survival of tumor plasma cells.[34,39] Here we suggested that syndecan-1 could be also involved in the modulation of the growth and survival of ECs within the BM microenvironment. In fact, knockdown of syndecan-1 expression by RNA interference resulted in arrest of the cell in G_2/M transition and M phase, and enhanced the sensitivity of MMECs to apoptosis. Moreover, in the present study we found that syndecan-1 expression correlated with enhanced *in vitro* and *in vivo* angiogenic activity. Indeed, downregulation of syndecan-1 was associated with a decreased *in vitro* capillary like-structure and *in vivo* angiogenic network
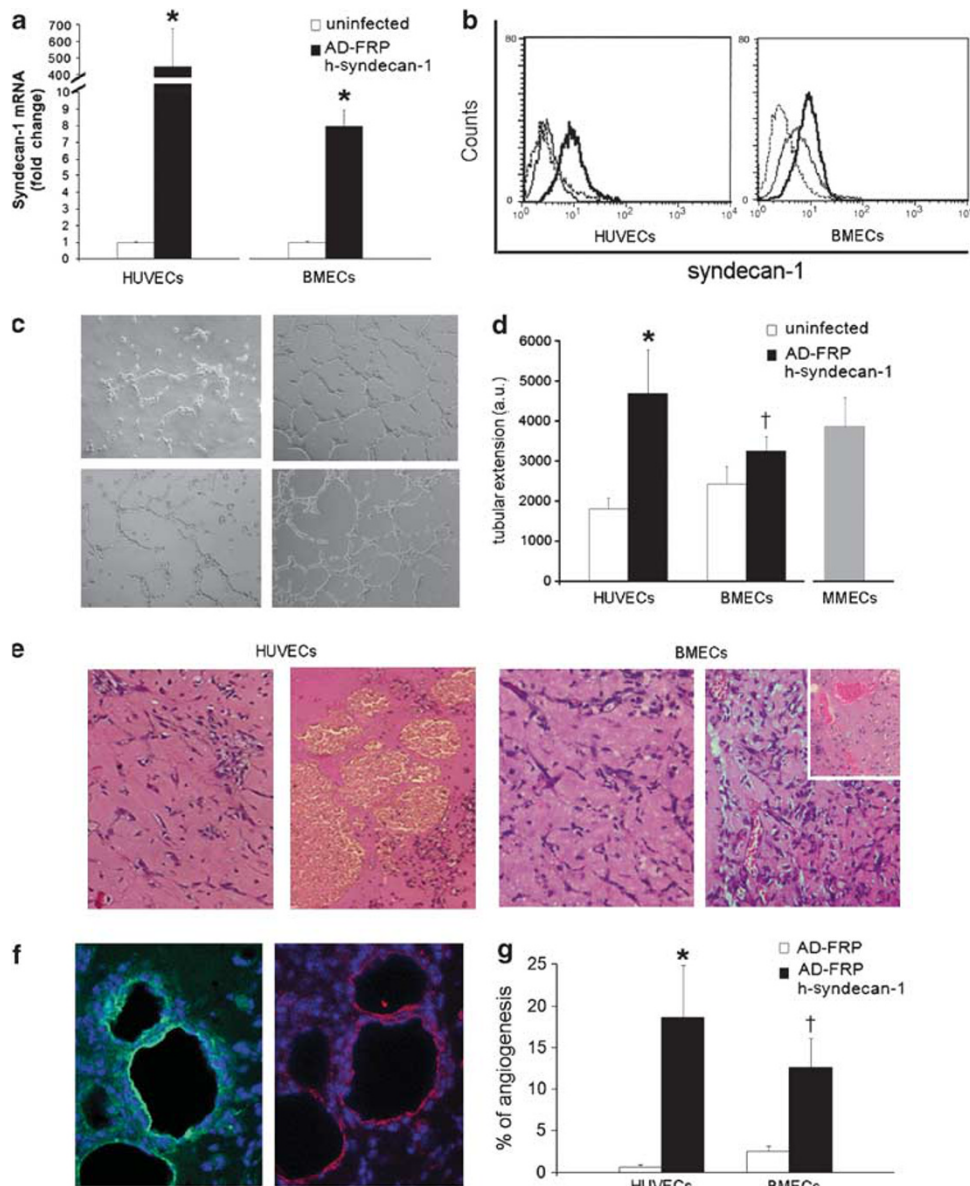
Figure 6. Syndecan-1 overexpression enhanced *in vitro* HUVEC and BMEC angiogenic ability. (**a**) Syndecan-1 mRNA level was analysed by qRT-PCR in AD-FRP h-syndecan-1 HUVECs or BMECs. The normalized expression of the *SDC1* gene with respect to *GAPDH* was computed for all samples. Uninfected HUVECs and BMECs were used as control (*$P < 0.05$ AD-FRP h-syndecan-1 HUVECs versus uninfected HUVECs; *$P < 0.01$ AD-FRP h-syndecan-1 BMECs versus uninfected BMECs). (**b**) Representative flow-cytometric histogram of syndecan-1 overexpression on HUVECs and BMECs. The thin line represents AD-FRP HUVECs or AD-FRP BMECs, infected with an empty adenovirus, and the dark line represents the AD-FRP h-syndecan-1 HUVECs or AD-FRP h-syndecan-1 BMECs, overexpressing syndecan-1; the dotted line represents the isotypic control. (**c**) Representative micrographs of capillary-like structure formation on Matrigel by uninfected HUVECs (top left), AD-FRP h-syndecan-1 HUVECs (top right), uninfected BMECs (bottom left) and AD-FRP h-syndecan-1 BMECs (bottom right) after 5 h. Original magnification, $\times 100$. (**d**) Morphometric evaluation of capillary-like structures formed onto Matrigel. Data are expressed as the mean ± s.d. of the length of capillary-like structures detected in five different fields of four different experiments performed in triplicate. Original magnification, $\times 100$. Analysis of variance with Newman–Keuls multi-comparison test was performed (*$P < 0.001$ AD-FRP h-syndecan-1 versus uninfected HUVECs; $^{†}P < 0.01$ AD-FRP h-syndecan-1 versus uninfected BMECs). (**e**) Representative micrographs of Matrigel-containing AD-FRP HUVECs (left), as control, and AD-FRP h-syndecan-1 HUVECs (right), and AD-FRP BMECs (left), as control, and AD-FRP h-syndecan-1 BMECs (right) injected subcutaneously into SCID mice. Original magnification, $\times 200$. The inset shows formation of aneurism-like structure by AD-FRP h-syndecan-1 BMECs. Original magnification, $\times 100$. (**f**) Representative confocal micrograph showing expression of human CD31 (bottom left) and human leukocyte antigen class-I (bottom right) on neo formed vessels within Matrigel by AD-FRP h-yndecan-1 HUVECs. Original magnification, $\times 400$. (**g**) Morphometric analysis of new formed vessels within Matrigel. Data are expressed as the mean ± s.d. of the length of capillary-like structures of five individual experiments. Only vascular structures containing red blood cells were counted as vessels. Original magnification, $\times 100$. Analysis of variance with Newman–Keuls multi-comparison test was performed (*$P < 0.001$ AD-FRP h-syndecan-1 versus AD-FRP HUVECs; $^{†}P < 0.001$ AD-FRP h-syndecan-1 versus AD-FRP BMECs).

formation. Thus, syndecan-1, promoting cell-to-cell interactions, stimulated MMEC organization into *in vitro* capillary-like structures and *in vivo* vessel formation. These results are in line with data

suggesting a physiological role of syndecan-1 in the formation of new vessels.[17,40] Moreover, after syndecan-1 knockdown we observed a decreased production of active MMP-2 and MMP-9
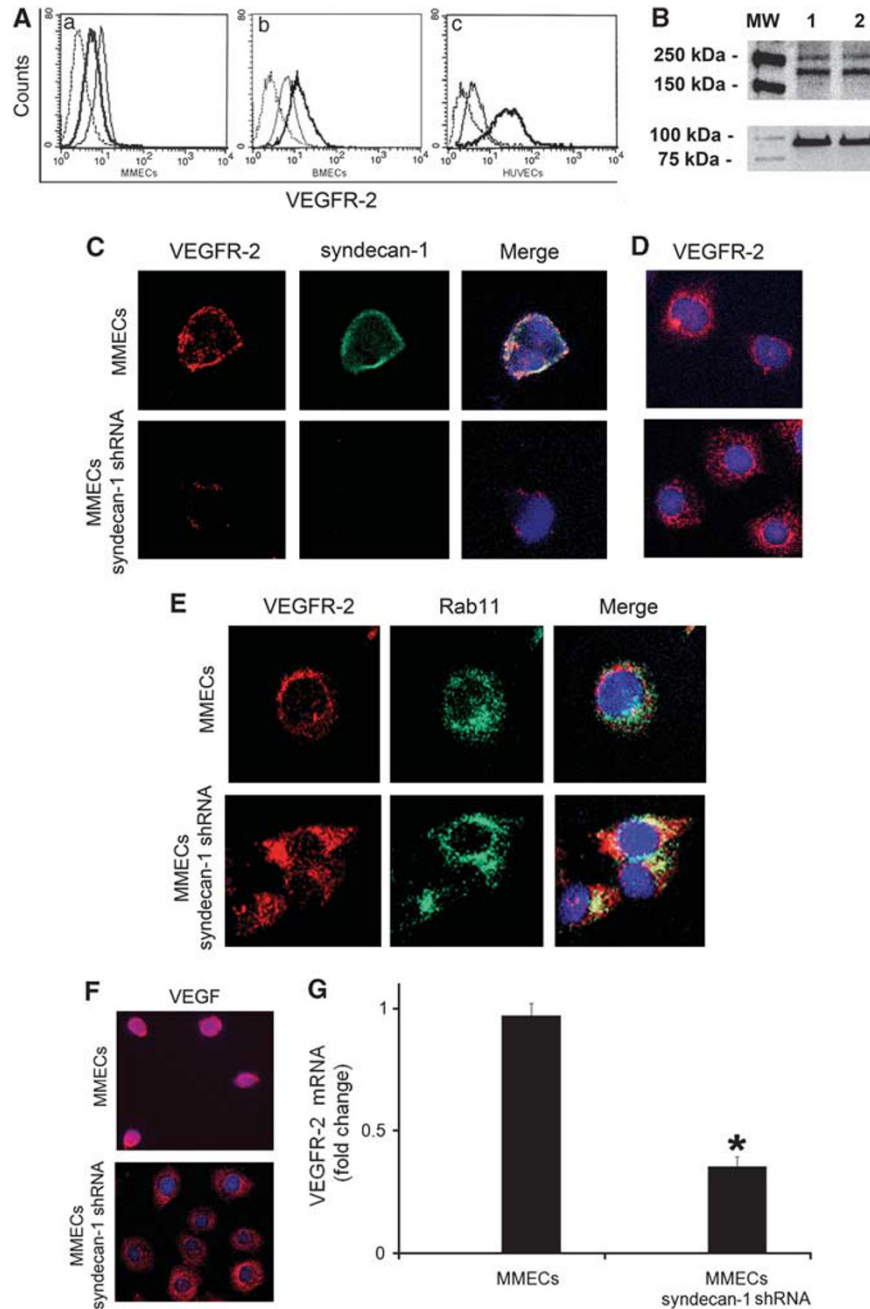
Figure 7. Syndecan-1 regulates VEGFR-2 expression. (**A**) Representative flow-cytometric analysis showing VEGFR-2 expression by (a) MMECs (thin line), MMEC syndecan-1 shRNA (dark line) and the corresponding isotype control antibody (dotted line); (b) BMECs (thin line), AD-FRP h-syndecan-1 BMECs (dark line) and the corresponding isotype control antibody (dotted line); and (c) HUVECs (thin line), AD-FRP h-syndecan-1 HUVECs (dark line) and the corresponding isotype control antibody (dotted lines). The flow-cytometric histograms are representative of three independent experiments with similar results. (**B**) Syndecan-1 immunoprecipitated with VEGFR-2. The immune complexes were formed by pre-incubation with anti-syndecan-1 and revealed with an antibody to VEGFR-2 (top), or by pre-incubation with anti-VEGFR-2 and revealed with an antibody to syndecan-1 (bottom). The data are from an individual experiment and are representative of two different lines of MMECs. (**C**) Representative confocal micrographs showing colocalization of VEGFR-2 and syndecan-1 on cellular membrane under the non-permeabilized condition (original magnification, × 630). (**D**) Representative confocal micrographs showing intracellular expression of VEGFR-2 in permeabilized cells (original magnification, × 630). (**E**) Representative confocal micrographs showing colocalization between VEGFR-2 and Rab11 in permeabilized cells (original magnification, × 630). (**F**) Representative confocal micrographs showing VEGFR-2 localization 30 min after stimulation with VEGF (25 ng/ml) (original magnification, × 630). (**G**) Comparison of VEGFR-2 mRNA expression between MMECs and MMEC syndecan-1 shRNA by qRT-PCR. The normalized expression of the genes with respect to *GAPDH* was computed for all samples. Values are expressed as fold change with respect to MMECs and are the mean ± s.d. of three independent experiments performed in triplicate. Student's *t*-test was performed (*$P < 0.001$ MMEC syndecan-1 shRNA versus MMECs).

by MMECs associated with a decrease of spontaneous Matrigel invasion. These results suggest that syndecan-1 can promote endothelial invasion into the extracellular matrix directly or indirectly regulating MMPs. We also showed decreased adherence of syndecan-1-knockdown MMECs to Matrigel. This result suggests that syndecan-1, by mediating also cell-to-matrix interactions,[34]
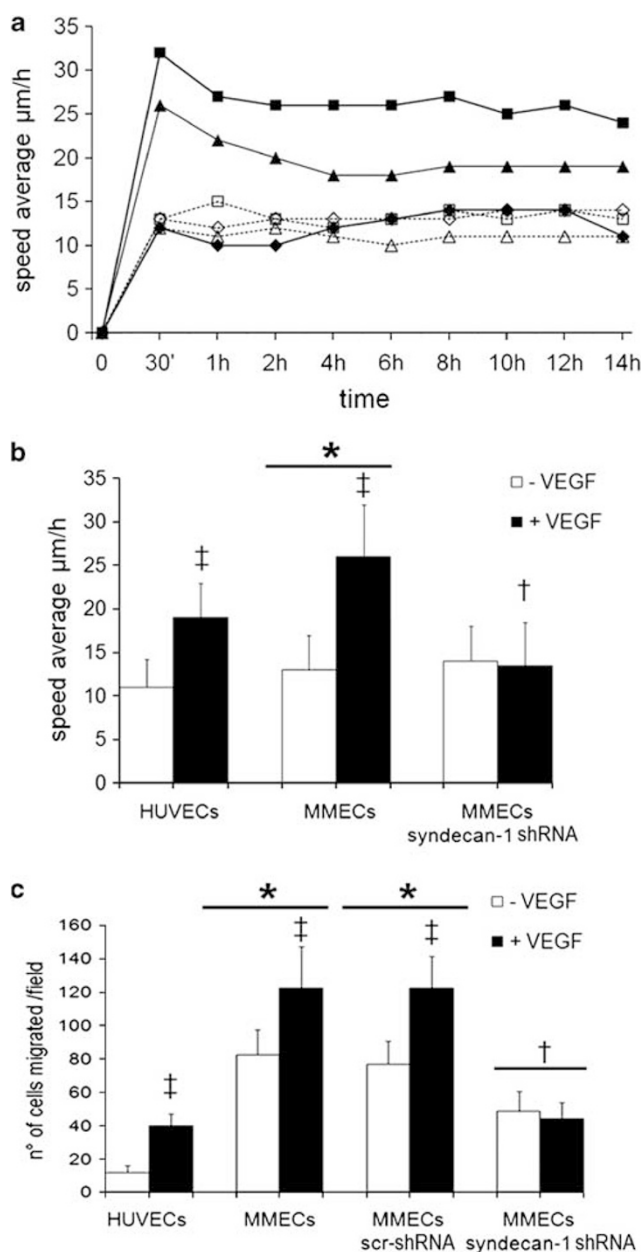
Figure 8. Syndecan-1 expression modulates VEGF-induced motility and migration. (**a**) Motility of HUVECs (▲), MMECs (■) and MMEC syndecan-1 siRNA (◆) in the presence (thin line) or absence (dotted line) of a VEGF stimulus (25 ng/ml) was monitored by time-lapse analysis for a period of 14 h and measured in μm/h as described under Materials and methods. (**b**) Speed average after 10 h of incubation in the presence (black bar) and absence (white bar) of a VEGF stimulus (25 ng/ml). The results are the mean ± s.d. of four individual experiments evaluating at least 30 cells for each experimental condition. Analysis of variance with Dunnett multiple comparison test was performed (*$P < 0.001$ MMECs versus HUVECs; †$P < 0.001$ MMEC syndecan-1 siRNA versus MMECs; ‡$P < 0.05$ VEGF stimulus (black bar) versus without VEGF stimulus (white bar)). (**c**) Invasion of HUVECs, MMECs and MMEC syndecan-1 siRNA towards Matrigel-coated filters was evaluated. VEGF (25 ng/ml) was added (black bar) or not added (white bar) to the lower chamber. Cells that migrated to the underside of the filters were counted in five microscope fields in each well. Original magnifications, × 100. Data are expressed as the mean ± s.d. of four independent experiments performed in duplicate. Analysis of variance with Dunnett multiple comparison test was performed (*$P < 0.001$ MMECs versus HUVECs; †$P < 0.001$ MMEC syndecan-1 siRNA versus MMECs; ‡$P < 0.001$ VEGF (black bar) versus without VEGF (white bar)).

promoted cell adhesion and invasion into the extracellular matrix. On the other hand, we demonstrated that acquisition by HUVECs and overexpression in BMECs of syndecan-1 induced a phenotype similar to that of MMECs. In fact, HUVECs and BMECs overexpressing syndecan-1 showed an enhanced ability to form capillary-like structure *in vitro*. Moreover, HUVECs and BMECs overexpressing syndecan-1 acquired a highly angiogenic phenotype when injected in Matrigel in SCID mice. These data suggest that syndecan-1 expression may influence the angiogenic behaviour of ECs contributing to the acquisition of an activated phenotype. This phenotype may depend not only on an enhanced cell-to-cell interaction and production of MMPs, but also on an enhanced response to pro-angiogenic factors. Indeed, comparing the MMEC phenotype versus that of syndecan-1-knockdown MMECs, we observed a decrease of VEGFR-2 surface expression. Immunoprecipitation studies demonstrated a physical interaction between syndecan-1 and VEGFR-2. This observation is consistent with the ability of syndecan-1 to interact with this growth factor receptor.[22,23] Moreover, we found that syndecan-1 silencing correlated with a reduced ability of MMECs to respond to VEGF. This may depend on a modulatory role of syndecan-1 on VEGFR-2 expression. Indeed, after syndecan-1 silencing reduced VEGFR-2 surface expression and its preeminent localization within the cytoplasm in association with the endosomal recycling compartments was observed. These results suggest that the syndecan-1 expression prevents the intracellular recycling of VEGFR-2 and is relevant for maintaining the receptor within the plasma membrane, thus allowing interaction with its ligand. Moreover, nuclear translocation of VEGFR-2 after interaction with VEGF,[41,42] which has been suggested to regulate its synthesis,[43] was almost completely absent in syndecan-1-knockdown cells. In agreement with this hypothesis, we observed a reduced expression of VEGFR-2 mRNA in syndecan-1-knockdown cells.

Previous studies demonstrated that syndecan-1 expression by plasma cells and its soluble form have a prognostic value.[16,30] Therefore, syndecan-1 has been considered a potential therapeutic target in MM. Several studies have successfully developed different syndecan-1 inhibition strategies.[35,37,38,44,45] A phase-I clinical study is ongoing using a cytotoxin-conjugated antibody against syndecan-1 (BT062).[46] The present finding that also MMECs express high levels of syndecan-1 with functional relevance in tumor angiogenesis extends the potential beneficial effect of syndecan-1 targeting against MM progression, acting both on the tumoral cell and the BM microenvironment. However, it remains to be determined whether syndecan-1 blockade might interfere with physiological angiogenesis. Further studies are needed to investigate whether syndecan-1 expression may define an angiogenic profile and correlate with cytogenetics and patient outcome.

In conclusion, the results of the present study provide a novel insight into regulation of MM angiogenesis by syndecan-1 and suggest that impairment of physiological function of syndecan-1 could be an interesting therapeutic approach for treatment of this malignancy.

CONFLICT OF INTEREST

The authors declare no conflict of interest.

DISCLAIMER

The authors alone are responsible for the content and writing of the paper.

REFERENCES

1 Kyle RA, Rajkumar SV. Multiple myeloma. *N Engl J Med* 2004; **351**: 1860–1873.

2 Jakob C, Sterz J, Zavrski I, Heider U, Kleeberg L, Fleissner C et al. Angiogenesis in multiple myeloma. *Eur J Cancer* 2006; **42**: 1581–1590.

3 Laroche M, Brousset P, Ludot I, Mazieres B, Thiechart M, Attal M. Increased vascularization in myeloma. *Eur J Haematol* 2001; **66**: 89–93.

4 Vacca A, Ribatti D. Bone marrow angiogenesis in multiple myeloma. *Leukemia* 2006; **20**: 193–199.

5 Sezer O, Niemoller K, Jakob C, Zavrski I, Heider U, Eucker J et al. Relationship between bone marrow angiogenesis and plasma cell infiltration and serum beta2-microglobulin levels in patients with multiple myeloma. *Ann Hematol* 2001; **80**: 598–601.

6 Pruneri G, Ponzoni M, Ferreri AJ, Decarli N, Tresoldi M, Raggi F et al. Microvessel density, a surrogate marker of angiogenesis, is significantly related to survival in multiple myeloma patients. *Br J Haematol* 2002; **118**: 817–820.

7 Rajkumar SV, Mesa RA, Fonseca R, Schroeder G, Plevak MF, Dispenzieri A et al. Bone marrow angiogenesis in 400 patients with monoclonal gammopathy of undetermined significance, multiple myeloma, and primary amyloidosis. *Clin Cancer Res* 2002; **8**: 2210–2216.

8 Vacca A, Ribatti D, Roncali L, Ranieri G, Serio G, Silvestris F et al. Bone marrow angiogenesis and progression in multiple myeloma. *Br J Haematol* 1994; **87**: 503–508.

9 Pellegrino A, Ria R, Di Pietro G, Cirulli T, Surico G, Pennisi A et al. Bone marrow endothelial cells in multiple myeloma secrete CXC-chemokines that mediate interactions with plasma cells. *Br J Haematol* 2005; **129**: 248–256.

10 Ria R, Todoerti K, Berardi S, Coluccia AM, De Luisi A, Mattioli M et al. Gene expression profiling of bone marrow endothelial cells in patients with multiple myeloma. *Clin Cancer Res* 2009; **15**: 5369–5378.

11 Vacca A, Ria R, Semeraro F, Merchionne F, Coluccia M, Boccarelli A et al. Endothelial cells in the bone marrow of patients with multiple myeloma. *Blood* 2003; **102**: 3340–3348.

12 Vacca A, Scavelli C, Serini G, Di Pietro G, Cirulli T, Merchionne F et al. Loss of inhibitory semaphorin 3A (SEMA3A) autocrine loops in bone marrow endothelial cells of patients with multiple myeloma. *Blood* 2006; **108**: 1661–1667.

13 Wijdenes J, Vooijs WC, Clement C, Post J, Morard F, Vita N et al. A plasmocyte selective monoclonal antibody (B-B4) recognizes syndecan-1. *Br J Haematol* 1996; **94**: 318–323.

14 Witzig TE, Kimlinger T, Stenson M, Therneau T. Syndecan-1 expression on malignant cells from the blood and marrow of patients with plasma cell proliferative disorders and B-cell chronic lymphocytic leukemia. *Leuk Lymphoma* 1998; **31**: 167–175.

15 Dhodapkar MV, Kelly T, Theus A, Athota AB, Barlogie B, Sanderson RD. Elevated levels of shed syndecan-1 correlate with tumour mass and decreased matrix metalloproteinase-9 activity in the serum of patients with multiple myeloma. *Br J Haematol* 1997; **99**: 368–371.

16 Seidel C, Sundan A, Hjorth M, Turesson I, Dahl IM, Abildgaard N et al. Serum syndecan-1: a new independent prognostic marker in multiple myeloma. *Blood* 2000; **95**: 388–392.

17 Iozzo RV, San Antonio JD. Heparan sulfate proteoglycans: heavy hitters in the angiogenesis arena. *J Clin Invest* 2001; **108**: 349–355.

18 Ruhrberg C, Gerhardt H, Golding M, Watson R, Ioannidou S, Fujisawa H et al. Spatially restricted patterning cues provided by heparin-binding VEGF-A control blood vessel branching morphogenesis. *Genes Dev* 2002; **16**: 2684–2698.

19 Cohen T, Gitay-Goren H, Sharon R, Shibuya M, Halaban R, Levi BZ et al. VEGF121, a vascular endothelial growth factor (VEGF) isoform lacking heparin binding ability, requires cell-surface heparan sulfates for efficient binding to the VEGF receptors of human melanoma cells. *J Biol Chem* 1995; **270**: 11322–11326.

20 Gitay-Goren H, Soker S, Vlodavsky I, Neufeld G. The binding of vascular endothelial growth factor to its receptors is dependent on cell surface-associated heparin-like molecules. *J Biol Chem* 1992; **267**: 6093–6098.

21 Yayon A, Klagsbrun M, Esko JD, Leder P, Ornitz DM. Cell surface, heparin-like molecules are required for binding of basic fibroblast growth factor to its high affinity receptor. *Cell* 1991; **64**: 841–848.

22 Chiang MK, Flanagan JG. Interactions between the Flk-1 receptor, vascular endothelial growth factor, and cell surface proteoglycan identified with a soluble receptor reagent. *Growth Factors* 1995; **12**: 1–10.

23 Dougher AM, Wasserstrom H, Torley L, Shridaran L, Westdock P, Hileman RE et al. Identification of a heparin binding peptide on the extracellular domain of the KDR VEGF receptor. *Growth Factors* 1997; **14**: 257–268.

24 Gambarini AG, Miyamoto CA, Lima GA, Nader HB, Dietrich CP. Mitogenic activity of acidic fibroblast growth factor is enhanced by highly sulfated oligosaccharides derived from heparin and heparan sulfate. *Mol Cell Biochem* 1993; **124**: 121–129.

25 Schlessinger J, Lax I, Lemmon M. Regulation of growth factor activation by proteoglycans: what is the role of the low affinity receptors? *Cell* 1995; **83**: 357–360.

26 Sanderson RD. Heparan sulfate proteoglycans in invasion and metastasis. *Semin Cell Dev Biol* 2001; **12**: 89–98.

27 Watanabe A, Mabuchi T, Satoh E, Furuya K, Zhang L, Maeda S et al. Expression of syndecans, a heparan sulfate proteoglycan, in malignant gliomas: participation of nuclear factor-kappaB in upregulation of syndecan-1 expression. *J Neurooncol* 2006; **77**: 25–32.

28 Beauvais DM, Burbach BJ, Rapraeger AC. The syndecan-1 ectodomain regulates alphavbeta3 integrin activity in human mammary carcinoma cells. *J Cell Biol* 2004; **167**: 171–181.

29 Conejo JR, Kleeff J, Koliopanos A, Matsuda K, Zhu ZW, Goecke H et al. Syndecan-1 expression is upregulated in pancreatic but not in other gastrointestinal cancers. *Int J Cancer* 2000; **88**: 12–20.

30 Khotskaya YB, Dai Y, Ritchie JP, MacLeod V, Yang Y, Zinn K et al. Syndecan-1 is required for robust growth, vascularization, and metastasis of myeloma tumors in vivo. *J Biol Chem* 2009; **284**: 26085–26095.

31 Maeda T, Alexander CM, Friedl A. Induction of syndecan-1 expression in stromal fibroblasts promotes proliferation of human breast cancer cells. *Cancer Res* 2004; **64**: 612–621.

32 Deambrosis I, Lamorte S, Giaretta F, Tei L, Biancone L, Bussolati B et al. Inhibition of CD40–CD154 costimulatory pathway by a cyclic peptide targeting CD154. *J Mol Med* 2009; **87**: 181–197.

33 Fonsato V, Buttiglieri S, Deregibus MC, Bussolati B, Caselli E, Di Luca D et al. PAX2 expression by HHV-8-infected endothelial cells induced a proangiogenic and proinvasive phenotype. *Blood* 2008; **111**: 2806–2815.

34 Sanderson RD, Sneed TB, Young LA, Sullivan GL, Lander AD. Adhesion of B lymphoid (MPC-11) cells to type I collagen is mediated by integral membrane proteoglycan, syndecan. *J Immunol* 1992; **148**: 3902–3911.

35 Post J, Vooijs WC, Bast BJ, De Gast GC. Efficacy of an anti-CD138 immunotoxin and doxorubicin on drug-resistant and drug-sensitive myeloma cells. *Int J Cancer* 1999; **83**: 571–576.

36 Ragnarsson L, Stromberg T, Wijdenes J, Totterman TH, Weigelt C. Multiple myeloma cells are killed by syndecan-1-directed superantigen-activated T cells. *Cancer Immunol Immunother* 2001; **50**: 382–390.

37 Tassone P, Goldmacher VS, Neri P, Gozzini A, Shammas MA, Whiteman KR et al. Cytotoxic activity of the maytansinoid immunoconjugate B-B4-DM1 against CD138+ multiple myeloma cells. *Blood* 2004; **104**: 3688–3696.

38 Yang Y, MacLeod V, Dai Y, Khotskaya-Sample Y, Shriver Z, Venkataraman G et al. The syndecan-1 heparan sulfate proteoglycan is a viable target for myeloma therapy. *Blood* 2007; **110**: 2041–2048.

39 Alexander CM, Reichsman F, Hinkes MT, Lincecum J, Becker KA, Cumberledge S et al. Syndecan-1 is required for Wnt-1-induced mammary tumorigenesis in mice. *Nat Genet* 2000; **25**: 329–332.

40 Sasisekharan R, Moses MA, Nugent MA, Cooney CL, Langer R. Heparinase inhibits neovascularization. *Proc Natl Acad Sci USA* 1994; **91**: 1524–1528.

41 Blazquez C, Cook N, Micklem K, Harris AL, Gatter KC, Pezzella F. Phosphorylated KDR can be located in the nucleus of neoplastic cells. *Cell Res* 2006; **16**: 93–98.

42 Santos SC, Dias S. Internal and external autocrine VEGF/KDR loops regulate survival of subsets of acute leukemia through distinct signaling pathways. *Blood* 2004; **103**: 3883–3889.

43 Jacinta S. Role of VEGF signalling in the regulation of KDR expression in endothelial and tumoral microenvironment. *BMC Proc* 2010; **4** (Suppl 2): 34.

44 Ikeda H, Hideshima T, Fulciniti M, Lutz RJ, Yasui H, Okawa Y et al. The monoclonal antibody nBT062 conjugated to cytotoxic maytansinoids has selective cytotoxicity against CD138-positive multiple myeloma cells in vitro and in vivo. *Clin Cancer Res* 2009; **15**: 4028–4037.

45 Reijmers RM, Groen RW, Rozemuller H, Kuil A, de Haan-Kramer A, Csikos T et al. Targeting EXT1 reveals a crucial role for heparan sulfate in the growth of multiple myeloma. *Blood* 2010; **115**: 601–604.

46 Lutz RJ, Whiteman KR. Antibody-maytansinoid conjugates for the treatment of myeloma. *MAbs* 2009; **1**: 548–551.

Supplementary Information accompanies the paper on the Leukemia website (http://www.nature.com/leu)